PHYSICAL REVIEW C **91**, 044910 (2015)

Hadron resonance gas and mean-field nuclear matter for baryon number fluctuations

Kenji Fukushima

Department of Physics, The University of Tokyo, 7-3-1 Hongo, Bunkyo-ku, Tokyo 113-0033, Japan

(Received 11 September 2014; revised manuscript received 3 April 2015; published 30 April 2015)

I give an estimate for the skewness and the kurtosis of the baryon number distribution in two representative models; i.e., models of a hadron resonance gas and relativistic mean-field nuclear matter. I emphasize formal similarity between these two descriptions. The hadron resonance gas leads to a deviation from the Skellam distribution if quantum statistical correlation is taken into account at high baryon density, but this effect is not strong enough to explain fluctuation data seen in the beam-energy scan at RHIC/STAR. In the calculation of mean-field nuclear matter, the density correlation with the vector ω field rather than the effective mass with the scalar σ field renders the kurtosis suppressed at higher baryon density so as to account for the experimentally observed behavior of the kurtosis. Finally, I discuss the difference between the baryon number and the proton number fluctuations from correlation effects in isospin space. The numerical results suggest that such effects are only minor even in the case of complete randomization of isospin.

DOI: 10.1103/PhysRevC.91.044910 PACS number(s): 25.75.Gz, 24.10.Pa, 21.65.−f

I. INTRODUCTION

The phase diagram of matter described by quantum chromodynamics (QCD) in terms of quarks and gluons, i.e., the QCD phase diagram, has not been unveiled yet in spite of tremendous theoretical and experimental efforts [1,2]. The most severe obstacle lies in the notorious sign problem which prevents the first-principle lattice QCD simulation from working at high baryon density, although there is steady progress to circumvent it [3]. There are so many theoretical speculations on the QCD phase structures but it is next to impossible to constrain them enough to pin down the right one or to eliminate unphysical ones. Even if there were a way to evade the sign problem, it would still be a highly nontrivial question whether the numerical simulation can correctly identify the genuine ground state if it includes a possibility of spatial modulation [4]. Taking the continuum limit and overcoming the discretization error should be crucial to resolve intricate structures such as the critical point [5] (see also Ref. [6] for a heuristic argument) and, if any, the crystalline condensates [7,8] (see Ref. [9] for an argument parallel to Ref. [6] and also Ref. [10] for a comprehensive review).

It is thus our hope that the experimental data should be able to constrain diverse candidates of the QCD phase diagram, so that we can identify the correct answer. Now that there is reasonable evidence of the formation of a new state of matter out of quarks and gluons, which is called the quark-gluon plasma, at sufficiently high energy, some of future heavy-ion collision programs are directed toward higher baryon density with lower collision energies. Such a project to explore the QCD phase diagram by tuning the collision energy is often called the beam-energy scan (BES) and the STAR Collaboration at the Relativistic Heavy Ion Collider (RHIC) already published the first BES (i.e., BES-I) results [11]. The primary mission of the BES was to discover the so-called QCD critical point by looking at fluctuations of conserved quantities such as the baryon number and the strangeness [5,12,13].

So far, there is no appreciable indication of the critical behavior,[1] and nevertheless, the BES has turned out to be extremely intriguing for QCD physics, for our understanding of finite-density QCD is severely limited and any hint would be useful. With accumulation of abundant experimental data, it might even be feasible to find a way for drastic simplification, leading to pragmatic modeling. We have already witnessed such a simplification in RHIC at high temperature T and low baryon chemical potential $\mu_{\rm B}$; the statistical thermal fit [14–16] and the hadron resonance gas (HRG) model (see Ref. [17] and references therein and also Ref. [18] for a recent study) stunningly reproduce the experimental yields of particles and are also consistent with lattice-QCD thermodynamics. Nobody believed in the reality of such an oversimplified description of noninteracting hadrons before the good agreement to experimental data was confirmed. Although the theoretical foundation needs more investigation, this expedient but profitable tool for data analysis is as effective for analyzing experimental data taken by the ALICE Collaboration at Large Hadron Collider (LHC) (see Ref. [19] and references therein), although minor deviations were reported.

We cannot, of course, trust the HRG model over the entire QCD phase diagram away from the chemical freeze-out line. It is obvious that the HRG should break down in the region of nuclear matter at low T and high $\mu_{\rm B}$. Nuclear physics at $T=0$ has revealed that a first-order liquid-gas phase transition (or liquid vacuum at $T=0$) should take place at $\mu_{\rm B}=M_N-B$ with M_N and B being the nucleon mass and the binding energy $B\simeq 16$ MeV [20]. Some years ago an interesting possibility was demonstrated [21]; the chemical freeze-out condition at

[1] A new analysis including higher-p_t data (that was motivated to improve the statistics) suggests critical behavior. It is still under dispute; I should note that, if $T\sim\Lambda_{\rm QCD}\sim 0.2$ GeV, the kinetic energy should be; $p_t^2/2m_{\rm N}\sim T/2$ leading to $p_t\sim 0.4$ GeV. It should be explained why higher-p_t data (above 0.8 GeV) enhance the criticality. So, in this work, I focus on the published data only.

low T and high $\mu_{\rm B}$ could be rather sensitive to nuclear matter properties. The present work aims to pursue the idea along the same line to show the agreement for not only the chemical freeze-out condition but also the fluctuations.

One might have an impression that the HRG is a sort of opposite to nuclear matter and that one should abandon the HRG immediately to switch to the nuclear physics terrain. This intuition is not totally correct, however, and we know that the independent quasiparticle picture makes good sense inside of nuclei and nuclear matter. Hence, on the formal level, the HRG-like model with "renormalized" parameters may have a chance to work continuously from low $\mu_{\rm B}$ to high $\mu_{\rm B}$. Indeed, the relativistic mean-field (RMF) model of nuclear matter is designed in this spirit. The simplest setup of the RMF is the σ-ω model [22] as was adopted in Ref. [21]. This model deals with nucleons as relativistic quasiparticles moving in the scalar mean field σ and the vector mean field ω. I note that we can safely neglect π fluctuations as long as we are concerned with the baryon number at small T. If needed, I can extend my present analysis so as to include π fluctuations; for example, with the renormalization group improvement [23].

This paper is organized as follows: I give a detailed description of fluctuations within the framework of the HRG model in Sec. II. Then, based on the similarity to the HRG model, I introduce the RMF model in Sec. III and I present my central numerical results from the RMF model in Sec. IV. In Sec. V I give more considerations on the microscopic structures of my numerical results. I also discuss the difference between the baryon number and the proton number to discover that the diffusion in isospin space does not affect my results as long as the Boltzmann approximation makes sense, which is addressed in Sec. VI. Finally, I summarize this work in Sec. VII.

II. FLUCTUATIONS AND HADRON RESONANCE GAS

First of all, before going into the descriptions of the HRG model, I should elucidate the physical observables of interest. I follow the standard convention used in Ref. [18] for thermal fluctuations which are derived from the derivatives of the pressure with respect to the relevant chemical potentials. For the baryon number fluctuation, thus, I calculate the following dimensionless quantities:

$$\chi_B^{(n)} \equiv \frac{\partial^n}{\partial\,(\mu_{\rm B}/T)^n}\frac{p}{T^4}, \tag{1}$$

from which I can construct the mean value (i.e., the particle number); $M \equiv VT^3\chi_B^{(1)}$. For an arbitrary distribution I can define the Gaussian width σ^2 together with the non-Gaussian fluctuations such as the skewness S and the kurtosis κ as [12,18]

$$\frac{\sigma^2}{M} \equiv \frac{\chi_B^{(2)}}{\chi_B^{(1)}}, \quad S\sigma \equiv \frac{\chi_B^{(3)}}{\chi_B^{(2)}}, \quad \kappa\sigma^2 \equiv \frac{\chi_B^{(4)}}{\chi_B^{(2)}}. \tag{2}$$

Therefore, once some theoretical estimates provide us with the pressure p as a function of $\mu_{\rm B}$, I can give a prediction for these fluctuations under an assumption of the dominance of thermal fluctuations.

Second, to make a contact with the collision experiment, it is necessary to relate the collision energy $\sqrt{s_{NN}}$ and T and $\mu_{\rm B}$. Fortunately, such a parametrization of $T(\sqrt{s_{NN}})$ and $\mu_{\rm B}(\sqrt{s_{NN}})$ has been well established along the chemical freeze-out line [14], which reads

$$T\,(\mu_{\rm B}) = a - b\mu_{\rm B}^2 - c\mu_{\rm B}^4, \tag{3}$$

$$\mu_{\rm B}(\sqrt{s_{NN}}) = \frac{d}{1+e\sqrt{s_{NN}}}, \tag{4}$$

where the parameters are chosen as $a = 0.166$ GeV, $b = 0.139$ GeV^{-1}, $c = 0.053$ GeV^{-3}, $d = 1.308$ GeV, and $e = 0.273$ GeV^{-1} to reproduce experimentally observed particle yields. Charge and strangeness chemical potentials, μ_Q and μ_S, are also parametrized in a similar manner. In my present analysis, I numerically checked that the inclusion of μ_Q and μ_S hardly changes the fluctuation results, so I neglect them for clarity of presentation. These definitions and parametrizations are robust and unchanged for any model applications.

Now I take a step toward the HRG model. Let us start with a simple demonstration of free nucleon gas and then proceed to the realistic HRG model next. In the estimate with noninteracting hadrons (in which the canonical factor γ is not included) I make use of the standard expression of the free grand canonical partition function. That is, the pressure from baryons (fermions) is prescribed as

$$p_{\rm free}(m_{\rm N},\mu_{\rm B}) = \sum_i^N 2T\int\frac{d^3p}{(2\pi)^3}\{\ln[1+e^{-(\varepsilon_p-\mu_{\rm B})/T}] + \ln[1+e^{-(\varepsilon_p+\mu_{\rm B})/T}]\}. \tag{5}$$

Here N is 2 for nucleons corresponding to the isospin degeneracy and the pressure depends on the nucleon mass $m_{\rm N}$ through the energy dispersion relation $\varepsilon_p \equiv (\boldsymbol{p}^2+m_{\rm N}^2)^{1/2}$. I can then take the derivatives of the above expression, which results in

$$\chi_B^{(n)} = \frac{4}{T^3}\int\frac{d^3p}{(2\pi)^3}X^{(n)}(p), \tag{6}$$

where the factor of four appears from the spin and the isospin degeneracy (for $N=2$) and the integrands read

$$\begin{aligned}
X^{(1)} &= n_p - \bar{n}_p,\\
X^{(2)} &= n_p(1-n_p) + \bar{n}_p(1-\bar{n}_p),\\
X^{(3)} &= n_p(1-n_p)(1-2n_p) - \bar{n}_p(1-\bar{n}_p)(1-2\bar{n}_p),\\
X^{(4)} &= \big(1-6n_p+6n_p^2\big)n_p(1-n_p)\\
&\quad + \big(1-6\bar{n}_p+6\bar{n}_p^2\big)\bar{n}_p(1-\bar{n}_p),
\end{aligned} \tag{7}$$

with $n_p \equiv [e^{(\varepsilon_p-\mu_{\rm B})/T}+1]^{-1}$ and $\bar{n}_p \equiv [e^{(\varepsilon_p+\mu_{\rm B})/T}+1]^{-1}$ being the Fermi–Dirac distribution functions for nucleons and antinucleons, respectively. I can continue taking the derivatives for even larger n if needed.

In the Boltzmann approximation, which is valid when n_p and $\bar{n}_p$ are both dilute, I can neglect the quantum statistical factors of nonlinear n_p and $\bar{n}_p$ terms. Then, I can approximate Eq. (7) because $X^{(2)} \approx X^{(4)} \approx (e^{\mu_{\rm B}/T}+e^{-\mu_{\rm B}/T})e^{-\varepsilon_p/T}$ and $X^{(3)} \approx (e^{\mu_{\rm B}/T}-e^{-\mu_{\rm B}/T})e^{-\varepsilon_p/T}$. In this particular limit I can

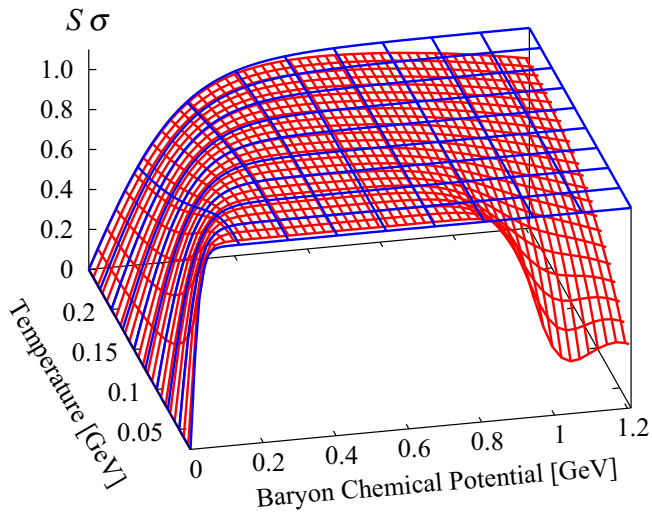

FIG. 1. (Color online) Skewness of the baryon number estimated in the HRG (THERMUS2.3) is shown by the (red) fine mesh. The (blue) sparse mesh represents the Skellam expectation, $\tanh(\mu_B/T)$.

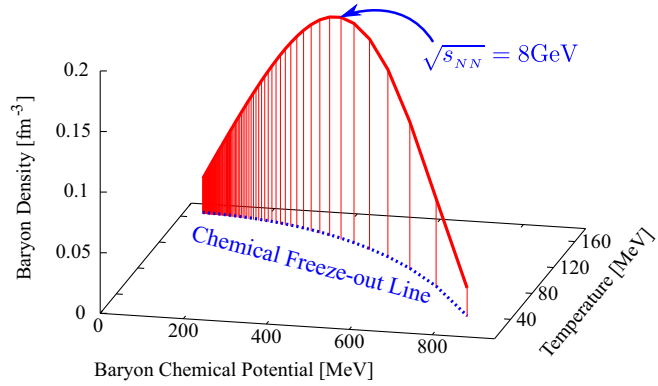

FIG. 3. (Color online) HRG-estimated baryon density (including not only nucleons but also all baryonic resonances of the particle data contained in the THERMUS2.3 package) as a function of T and μ_B. The nucleon contribution is nearly a half of the results shown. The vertical lines represent the collision energy with spacing of 1 GeV. The extremal point corresponds to $\sqrt{s_{NN}} \simeq 8$ GeV. The chemical freeze-out line is drawn according to Eqs. (3) and (4).

readily derive

$$S\sigma = \tanh(\mu_B/T), \quad \kappa\sigma^2 = 1, \tag{8}$$

which are nothing but the Skellam expectations. I can easily generalize the above derivation of Eq. (8) to a superposition of arbitrary N with different masses to find that Eq. (8) still holds after all. This is because $e^{\mu_B/T} \pm e^{-\mu_B/T}$ is always factored out and the remaining integrand is common for $X^{(2)}$, $X^{(3)}$, and $X^{(4)}$.

Let us then quantify the breakdown of the Boltzmann approximation explicitly by scanning the three-dimensional (3D) landscape of $S\sigma$ and $\kappa\sigma^2$ for various T and μ_B. In Figs. 1 and 2 we show our results from (not a free nucleon gas but) the HRG model by using the particle data contained

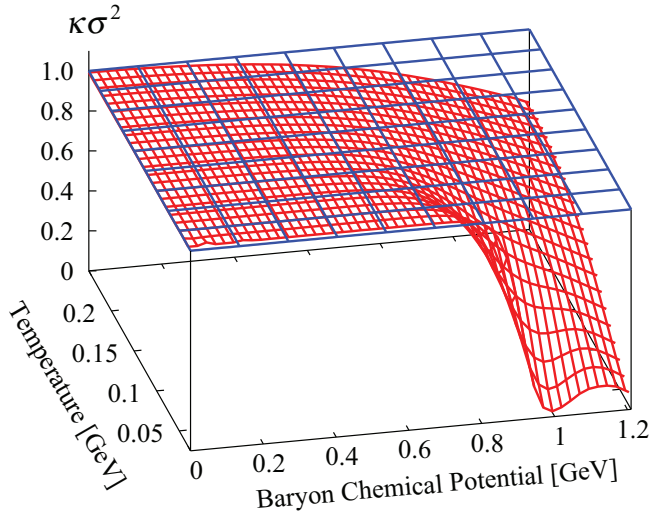

FIG. 2. (Color online) Kurtosis of the baryon number estimated in the HRG (THERMUS2.3) is shown by the (red) fine mesh. The (blue) sparse mesh represents the Skellam expectation, which is unity.

in the THERMUS2.3 package (by red fine mesh) as well as the Skellam predictions (by blue sparse mesh). It is clear from the figures that the quantum correlation certainly suppresses both $S\sigma$ and $\kappa\sigma^2$ in the high-density region where n_p is not really dilute. I should note that the HRG model can describe the onset behavior of finite baryon density but does not have dynamics enough to realize a first-order liquid-gas phase transition of nuclear matter (and this is why I do not show HRG results at temperatures smaller than a few tens of MeV in Figs. 1 and 2). Although this suppression effect is noticeable along the chemical freeze-out line as in Figs. 4 and 5, it is not sufficiently strong for reproducing the trend of the experimental data. In short, the quantum correlation is weak, as correctly speculated in Ref. [18], because the baryon density never gets large enough on the chemical freeze-out line.

To have a feeling about how the baryon density behaves on the chemical freeze-out line, I plot the integrated baryon density in the standard unit of fm^{-3} in Fig. 3. The vertical thin lines correspond to the collision energy $\sqrt{s_{NN}}$ with a spacing of 1 GeV. The lowest collision energy in Fig. 3 starts with $\sqrt{s_{NN}} = 2$ GeV, and the maximum of the baryon density is found at $\sqrt{s_{NN}} \sim 8$ GeV. It is interesting that this maximum position precisely coincides with the triple-point-like region as speculated in Ref. [24]. This coincidence is not accidental; in Ref. [24] the triple-point-like region was recognized based on the horn structure in K^+/π^+, which is sensitive to the strangeness chemical potential μ_S. If the bulk system maintains zero strangeness, it is not hard to confirm that μ_S is almost proportional to μ_B within an effective model framework [25]. In this way, naturally, K^+/π^+, Λ/π^-, Ξ/π^-, etc. have a peaked structure at $\sqrt{s_{NN}} \simeq 8$ GeV with which the baryon density is maximized.

As a final related remark I point out that the effect of the strangeness and the charge conservation is only of a few percent in $S\sigma$ and $\kappa\sigma^2$ along the chemical freeze-out line. I have checked this numerically by adopting μ_Q and μ_S parametrized along the chemical freeze-out line [18]. I then

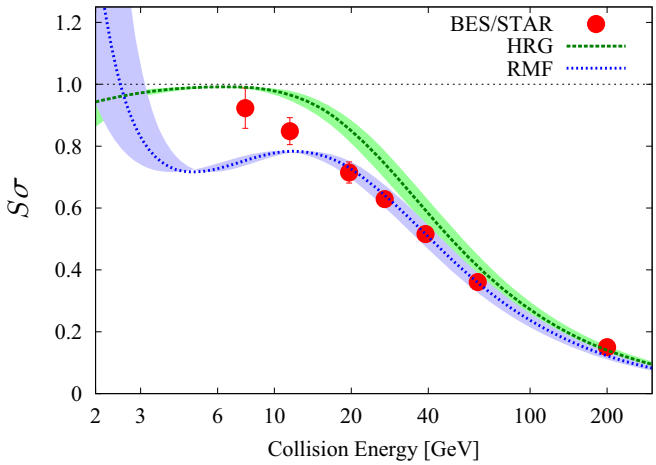

FIG. 4. (Color online) Skewness of the baryon number distribution. The red dot, the green dotted line, and the blue dashed line represent the results from the BES-STAR, the HRG, and the RMF, respectively. The bands represent uncertainty from the freeze-out μ_B by $\pm 10\%$.

observed that $S\sigma$ and $\kappa\sigma^2$ in Figs. 4 and 5 are pushed down by a few percent at most compared with the current $\mu_Q = \mu_S = 0$ case. This check justifies my discussion without μ_Q and μ_S taken into account.

III. SIMILARITY BETWEEN HADRON RESONANCE GAS AND RELATIVISTIC MEAN FIELD

Nuclear matter (which is a self-bound system of infinite nucleons) lies at the opposite limit to the noninteracting matter described by the HRG model. Nevertheless, theoretically speaking, the formulation of nuclear matter, namely the RMF, is not so far from the HRG model or they actually share similarity to some extent.

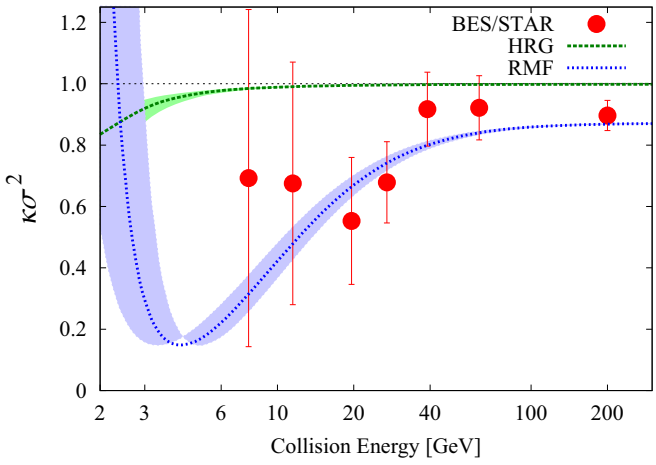

FIG. 5. (Color online) Kurtosis of the baryon number distribution. The legend convention is the same as in Fig. 4. The bands represent uncertainty from the freeze-out μ_B by $\pm 10\%$.

The simplest RMF is known as the σ-ω model defined by the partition function

$$p = (2)2T \int \frac{d^3p}{(2\pi)^3} \{\ln[1 + e^{-(\varepsilon_p - \mu_B^*)/T}] + \ln[1 + e^{-(\varepsilon_p + \mu_B^*)/T}]\} - \frac{m_\sigma^2 \sigma^2}{2} + \frac{m_\omega^2 \omega^2}{2}, \quad (9)$$

where the quasiparticle dispersion relation is $\varepsilon_p \equiv (\boldsymbol{p}^2 + m_N^{*2})^{1/2}$. Here, quantities with an asterisk are "in-medium" or "renormalized" quantities which contain a shift by the mean field as

$$m_N^* \equiv m_N - g_\sigma \sigma, \quad \mu_B^* \equiv \mu_B - g_\omega \omega. \quad (10)$$

These mean fields of σ and ω, or equivalently, m_N^* and μ_B^* are determined with the stationary conditions $\partial\Omega/\partial\sigma = \partial\Omega/\partial\omega = 0$, which lead to the gap equations. By choosing the model parameters appropriately [26]; i.e., $m_N = 939$ MeV, $m_\sigma = 550$ MeV, $m_\omega = 783$ MeV, $g_s = 10.3$, $g_\omega = 12.7$, we can reproduce the saturation properties of symmetric nuclear matter with the saturation density given by 0.17 nucleons/fm^3 and the binding energy per nucleon given by 16.3 MeV. I note that this simplest σ-ω model fails in reproducing the empirical value of the compressibility of symmetric nuclear matter [27]. It is possible to overcome this problem by extending the model with the self-coupling potential of the mean fields. For the fluctuations of my present interest, however, such improvement of the model makes only minor modifications to the final results [28]. This also implies that a different choice of m_σ, e.g., 500 MeV would not change the final results because g_s and g_ω should be readjusted to reproduce the saturation density and the binding energy, and so the difference would be the compressibility only.

From Eq. (9) it is obvious that the RMF estimate should reduce to nothing but the HRG estimate or Eq. (5) if I freeze the implicit dependence on μ_B through the solutions of σ and ω or, equivalently, m_N^* and μ_B^*. In this sense we can interpret the RMF treatment as a variation of the HRG model augmented with mean fields. Unlike the HRG model, however, the mean fields have an implicit dependence on μ_B, from which I should anticipate nontrivial contributions for the fluctuations.

In closing this section, I make an explicit statement about the validity regions of the HRG model and the RMF models. The HRG model is the most successful at the top energy of the RHIC, but the agreement of the thermal model fit to the experimental data becomes slightly worse for the LHC data. There is no clear explanation for this, but it is conceivable that the HRG model works the best near the crossover region of deconfinement. The meson sector of the HRG model is a valid picture in a fictitious world of $N_c \to \infty$ with which meson interactions would be turned off. The baryon sector behaves differently, however, and so the HRG model should naturally break down at high baryon density. A conservative estimate for this would suggest a validity region, $\mu_B < T$, that corresponds to $\sqrt{s_{NN}} \gtrsim 10$ GeV. On the other hand, the RMF model is supposed to describe nuclear matter which is reached at small $\sqrt{s_{NN}}$, and the validity region is limited by my approximation of neglecting pion fluctuations. Although the effect of pions is indirect for the baryon number fluctuations,

it could make a quantitative modification if the temperature is comparable to the pion mass. This condition would translate into the validity region $\sqrt{s_{NN}} \lesssim 10$ GeV in the energy unit. So, one may well expect that the HRG model at high energy should be taken over smoothly by the RMF model in the intermediate energy $\sqrt{s_{NN}} \sim 10$ GeV, which could be of course understood as another manifestation of the triple-point-like region [24].

IV. CENTRAL NUMERICAL RESULTS

Figures 4 and 5 show my results for $S\sigma$ and $\kappa\sigma^2$ estimated in the HRG (green dotted line) and in the RMF (blue dashed line) on top of the BES-STAR data (red dots). I note that the parametrization of the chemical freeze-out line, Eqs. (3) and (4), may have some uncertainty particularly at small $\sqrt{s_{NN}}$. To quantify the sensitivity I varied μ_B by $\pm 10\%$ to add the band on each line in Figs. 4 and 5. Now let me briefly discuss in particular two of the nontrivial features noticeable in these figures.

One feature is that the HRG model may have a richer structure than the Skellam distribution. Actually, it was clearly stated in Ref. [18] that the Skellam predictions come from the Boltzmann approximation. If the baryon density gets large, therefore, one naturally expects modifications on the distribution. More specifically, as seen in Figs. 4 and 5, the kurtosis is not necessarily unity at small $\sqrt{s_{NN}}$. This effect is not so substantial, but it would be interesting to reveal how the quantum correlation would affect the distribution in a wider region away from the chemical freeze-out line.

The other feature is that $\kappa\sigma^2$ in the RMF is suppressed at smaller $\sqrt{s_{NN}}$ thus larger μ_B. In fact the RMF-estimated $\kappa\sigma^2$ happens to approach the experimental data. It is, of course, the interaction effect that modifies $S\sigma$ and $\kappa\sigma^2$. Then, an immediate question that comes to my mind is which of σ and ω should be more responsible for the suppression seen in Fig. 5. One may well consider that, the in-medium effective mass can bring about the leading effect of the interactions, which is indeed the case whenever the Hartree approximation works. In the present problem, as we will see in the next section, the situation is rather involved. Because I take the μ_B derivatives to compute the baryon fluctuations, it turns out to be μ_B^* and thus ω that play the essential role for forming a peculiar shape of $\kappa\sigma^2$ in Fig. 5. Therefore, my study, as I will explain later, brings me to conclude that the renormalization of μ_B caused by ω suppresses $\kappa\sigma^2$, while the in-medium mass coupled with σ does the opposite. I comment that, in view of Figs. 4 and 5, the fluctuations grow again when $\sqrt{s_{NN}}$ reaches below $\sim$4 GeV. This low-$\sqrt{s_{NN}}$ enhancement of the fluctuations is simply because of the criticality when the chemical freeze-out line hits the liquid-gas critical point of nuclear matter [29] that is located at $T \simeq 21$ MeV and $\mu_B \simeq 906$ MeV in my RMF setup.

V. WHAT CAUSES THE SUPPRESSION?

As I mentioned previously, if I fix m_N^* and μ_B^* at the vacuum values; i.e., m_N and μ_B, and then take the μ_B derivatives, the results for $S\sigma$ and $\kappa\sigma^2$ are identical to what is referred to by the HRG in Figs. 4 and 5, which I have numerically checked. They

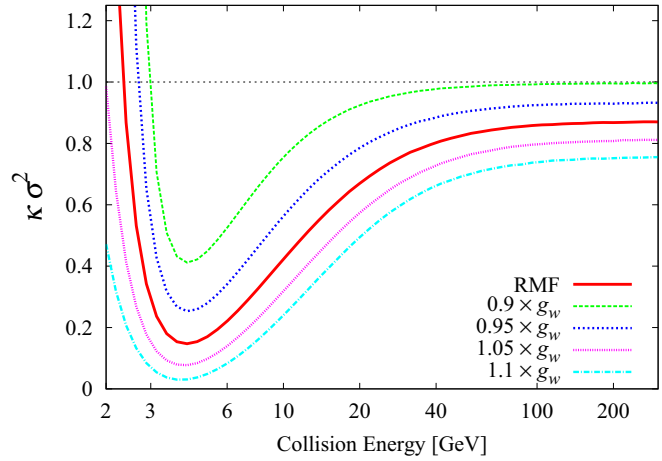

FIG. 6. (Color online) Kurtosis calculated in the RMF for various vector couplings.

are not exactly the same because the genuine HRG results have contributions also from higher baryonic resonances.

If I include the in-medium mass effect only, the μ_B derivative hits the implicit dependence in n_p and $\bar{n}_p$ and, for example, the first derivative reads

$$\frac{\partial n_p}{\partial(\mu_B/T)} = (1-\varepsilon_p')n_p(1-n_p) \simeq (1-\varepsilon_p')n_p \qquad (11)$$

in the Boltzmann approximation. Here, ε_p' represents $\partial\varepsilon_p/\partial\mu_B$. I find a similar expression for $\bar{n}_p$ with an overall minus sign and with $-\varepsilon_p'$ changed to $+\varepsilon_p'$.

At high density I can neglect the antiparticle contribution from $\bar{n}_p$ and, moreover, ε_p' is negative because the effective mass m_N^* generally decreases with increasing density. This means that $\partial n_p/\partial(\mu_B/T)$ is *greater* than n_p by an enhancement factor $1-\varepsilon_p' > 1$. In the approximation to neglect higher derivatives in terms of μ_B, therefore, $S\sigma$ and $\kappa\sigma^2$ should get larger, respectively, by $(1-\varepsilon_p')^3$ and $(1-\varepsilon_p')^4$.

In contrast to this behavior of m_N^*, the effect of the renormalized chemical potential μ_B^* yields a suppression factor by $\partial\mu_B^*/\partial\mu_B = 1 - g_\omega(\partial\omega/\partial\mu_B)$ where ω is proportional to the baryon density, so that I can conclude that $\partial\omega/\partial\mu_B > 0$. The above-mentioned arguments have been carefully confirmed in my numerical calculations.

Let us see the numerical check from a different viewpoint. I change the strength of the vector coupling g_ω by hand to find that $\kappa\sigma^2$ is certainly modified in a way consistent with the above qualitative arguments, as is transparent in Fig. 6; the entire curve goes down for larger g_ω. I should note, however, that I cannot infer g_ω from a fit of the model results to the experimental data. This is because I simply vary g_ω not adjusting other parameters to reproduce the saturation properties of nuclear matter. In this sense, thus, my results in Fig. 6 should not be regarded as anything beyond a test.

VI. EFFECTS OF ISOSPIN CORRELATIONS

So far, I have discussed a quantitative comparison assuming that the experimentally measurable quantities of the proton

number fluctuations are somehow to be identified as the baryon number fluctuations. One may wonder if it really works or not. In fact, such identification requires a nontrivial assumption about independence between neutrons and protons as is the case in the HRG calculation. One can readily understand this by expanding higher powers of $N_B = N_p + N_n$ where N_p and N_n are, respectively, the (net) proton number and the (net) neutron number. For the simplest example, the quadratic fluctuation consists of

$$\chi_B^{(2)} = \frac{1}{VT^3}\left(\langle N_B^2\rangle - \langle N_B\rangle^2\right) = \chi_p^{(2)} + \chi_n^{(2)} + 2\chi_{pn}^{(2)}, \quad (12)$$

where

$$\chi_{pn}^{(2)} \equiv \frac{1}{VT^3}(\langle N_p N_n\rangle - \langle N_p\rangle\langle N_n\rangle). \quad (13)$$

If the proton and the neutron behave independently from their isospin partners, there is no connected contribution in the correlation function of N_p and N_n; i.e., $\langle N_p N_n\rangle = \langle N_p\rangle\langle N_n\rangle$ and the last term involving $\chi_{pn}^{(2)}$ in Eq. (12) vanishes. As long as I do not consider isospin symmetry violation, the neutron fluctuation should be just identical with the proton fluctuation, so that I can conclude $\chi_B^{(2)} = 2\chi_p^{(2)}$ immediately from Eq. (12). I can continue similar arguments to deduce that $\chi_B^{(n)} = 2\chi_p^{(n)}$ in general. Therefore, obviously, this factor of two is canceled out in the dimensionless ratios and $S\sigma$ and $\kappa\sigma^2$ of protons take the same value as those of baryons (nucleons).

This argument is valid as long as I consider a free gas of baryons only. It is known, however, that off-diagonal components of the susceptibility such as $\chi_{ud} \propto \chi_{pn}^{(2)}$ are nonvanishing as observed in the lattice-QCD simulation [30] as well as in the model studies [31,32]. I do not go into technical details here but simply note that nonzero χ_{ud} is induced by different behavior of the Polyakov loop and the anti-Polyakov loop in a finite-density environment described by the Polyakov-loop extended Nambu–Jona–Lasinio model [33,34]. Physically speaking, different flavors communicate with each other through confining gluons to form pions. It is important to mention that χ_{ud} itself is finite also in the HRG calculation, which is attributed to pions rather than baryons. Then, a nonzero $\chi_{pn}^{(2)}$ of baryons should be induced by $\chi_{ud} \neq 0$ after all. Since I cannot avoid relying on another assumption to give a concrete estimate of induced $\chi_{pn}^{(2)}$, I shall postpone numerical analyses along this line to another presentation.

Recently, a more dynamical origin of isospin correlations has been discussed in Ref. [35]. That is, residual interactions after the chemical freeze-out can change p into n and vice versa. Of course, in the first approximation, I do not have to think of weak processes because the lifetime of matter in the heavy-ion collision is of order of the strong interaction. Still, such a mixing between $p \leftrightarrow n$ is allowed by the strong interaction involving π^0 and π^- through an intermediate state of $\Delta^+(1232)$ and $\Delta^0(1232)$. It should be a quite complicated procedure to establish any reliable evaluation for these contributions to $\chi_{pn}^{(2)}$, but I can drastically simplify the theoretical calculation in the limit of complete mixing or randomization, which is the limit opposite to complete independence in isospin space.

In this special case of complete randomization of isospin, it is a natural anticipation to presume that each (anti-) nucleon is either a (anti-) proton or a (anti-) neutron with equal probability. Therefore, the distribution of $\mathcal{N}_p$ is binomial with the mean value given by $\mathcal{N}_B/2$ [35], where $\mathcal{N}_p$ and $\mathcal{N}_B$ are not the net quantities but the *absolute* proton number and the *absolute* baryon (nucleon) number. That is, $N_p = \mathcal{N}_p - \mathcal{N}_{\bar{p}}$, $N_B = \mathcal{N}_B - \mathcal{N}_{\bar{B}}$, etc. Thus, for a given $\mathcal{N}_B$ and $\mathcal{N}_{\bar{B}}$ (for which the average is denoted by $\langle\cdots\rangle_B$), I expect

$$\bar{\mathcal{N}}_p = \langle\mathcal{N}_p\rangle_B = \tfrac{1}{2}\mathcal{N}_B, \quad (14)$$

$$\langle(\mathcal{N}_p - \bar{\mathcal{N}}_p)^2\rangle_B = \tfrac{1}{4}\mathcal{N}_B, \quad (15)$$

$$\langle(\mathcal{N}_p - \bar{\mathcal{N}}_p)^3\rangle_B = 0, \quad (16)$$

$$\langle(\mathcal{N}_p - \bar{\mathcal{N}}_p)^4\rangle_B = \tfrac{1}{16}\mathcal{N}_B(3\mathcal{N}_B - 2), \quad (17)$$

and so on according to the binomial distribution. I note that Eqs. (14)–(17) are T independent, unlike the thermal distribution.

I am now ready to express the proton number fluctuations in terms of baryon number fluctuations. For nth-order fluctuations I have

$$\chi_p^{(n)} = \frac{1}{VT^3}\left\langle\!\!\left\langle\left\langle\left(\mathcal{N}_p - \mathcal{N}_{\bar{p}} - \left\langle\!\!\left\langle\frac{\mathcal{N}_B - \mathcal{N}_{\bar{B}}}{2}\right\rangle\!\!\right\rangle\right)^n\right\rangle_B\right\rangle\!\!\right\rangle, \quad (18)$$

where $\langle\!\langle\cdots\rangle\!\rangle$ represents an average over the distribution of $\mathcal{N}_B$ and $\mathcal{N}_{\bar{B}}$.

By using these relations I can easily prove, for example, the following of the quadratic ($n = 2$) fluctuation:

$$\chi_p^{(2)} = \frac{1}{4}\chi_B^{(2)} + \frac{1}{4VT^3}\langle\!\langle\mathcal{N}_B + \mathcal{N}_{\bar{B}}\rangle\!\rangle, \quad (19)$$

where I used independence of the baryon and the antibaryon distributions. It should be noted that Eq. (19) exactly coincides with the formula derived in Ref. [35].

Let us see how large the second term could be; and for this purpose, I make use of an expression for the free baryon gas. Then, I numerically confirm that this second term is very close to the first term at good precision; i.e., $\langle\!\langle\mathcal{N}_B + \mathcal{N}_{\bar{B}}\rangle\!\rangle \approx \chi_B^{(2)}$ within 1% at large $\sqrt{s_{NN}}$ and at most 5% at smaller $\sqrt{s_{NN}}$ of a few GeV. I can then approximate $\chi_p^{(2)}$ as $\chi_p^{(2)} \approx (1/2)\chi_B^{(2)}$. This means that both Eq. (19) and the previous relation in the HRG model eventually lead to the same answer; $\chi_p^{(2)} = (1/2)\chi_B^{(2)}$ after all, although they superficially look quite different from each other.

I next proceed to the $n = 3$ case. Then, after some calculations, I can arrive at

$$\chi_p^{(3)} = \frac{1}{8}\chi_B^{(3)} + \tfrac{3}{8}\left(\mathcal{X}_B^{(2)} - \mathcal{X}_{\bar{B}}^{(2)}\right), \quad (20)$$

where I defined $\mathcal{X}_B^{(2)}$ and $\mathcal{X}_{\bar{B}}^{(2)}$ as

$$\mathcal{X}_B^{(2)} \equiv \frac{1}{VT^3}\left(\langle\!\langle\mathcal{N}_B^2\rangle\!\rangle - \langle\!\langle\mathcal{N}_B\rangle\!\rangle^2\right), \quad (21)$$

$$\mathcal{X}_{\bar{B}}^{(2)} \equiv \frac{1}{VT^3}\left(\langle\!\langle\mathcal{N}_{\bar{B}}^2\rangle\!\rangle - \langle\!\langle\mathcal{N}_{\bar{B}}\rangle\!\rangle^2\right). \quad (22)$$

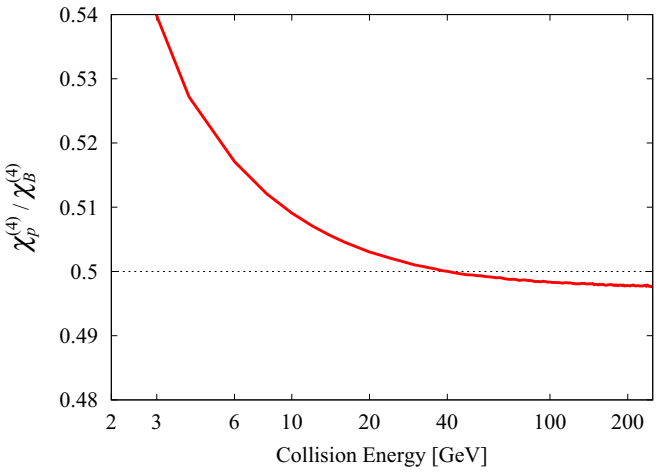

FIG. 7. (Color online) Ratio of $\chi_p^{(4)}$ to $\chi_B^{(4)}$ which is close to 1/2 and the deviation from 1/2 is less than 10% at small $\sqrt{s_{NN}}$.

So, the ordinary quadratic fluctuation is given as $\chi_B^{(2)} = \mathcal{X}_B^{(2)} + \mathcal{X}_{\bar{B}}^{(2)}$. My result above is again equivalent to the formula listed in Ref. [35]. It is also easy to check that this latter term in Eq. (20) gives the same answer as $\chi_B^{(3)}$ within a few percent as long as the baryon distribution is thermal. Therefore, $\chi_p^{(3)} \approx (1/2)\chi_B^{(3)}$ follows.

Now I can make a guess that probably $\chi_p^{(4)} \approx (1/2)\chi_B^{(4)}$ again and let us explicitly make it sure. In the same way I can write $\chi_p^{(4)}$ as

$$\chi_p^{(4)} = \frac{1}{16}\chi_B^{(4)} + \frac{3}{8}\left(\mathcal{X}_B^{(3)} + \mathcal{X}_{\bar{B}}^{(3)}\right) + \frac{3}{16}\chi_B^{(2)} - \frac{1}{8VT^3}\langle\langle \mathcal{N}_B + \mathcal{N}_{\bar{B}} \rangle\rangle. \quad (23)$$

This is indeed close to $(1/2)\chi_B^{(4)}$ but shows a deviation as $\sqrt{s_{NN}}$ gets smaller. I present our numerical results in Fig. 7. It is clear from Fig. 7 that $\chi_p^{(4)} \approx (1/2)\chi_B^{(4)}$ is the case as long as $\sqrt{s_{NN}}$ is sufficiently large, while it increases by about 10% at smaller $\sqrt{s_{NN}}$. My conclusion is that, contrary to what is claimed in Ref. [35], the isospin correlation does not help us with explaining a suppression tendency in the kurtosis at smaller $\sqrt{s_{NN}}$; the effect is in a wrong direction. In any case, the 10% correction is just too minor to account for almost 50% suppression in the experimental data as seen in Fig. 5.

Here I make a remark that I can easily give a general proof of $\chi_p^{(n)} \approx (1/2)\chi_B^{(n)}$ if I can make the Boltzmann approximation for the baryon distribution. Therefore, in this sense, the 10% deviation seen in Fig. 7 can be attributed to the violation of the Boltzmann approximation that is quantified by the deviation from unity in Fig. 5, which is also of the 10% level. The bottom line of my analysis is that I can safely neglect the difference between the baryon number and the proton number fluctuations.

VII. SUMMARY

I investigated the baryon number fluctuations by using the hadron resonance gas model and the mean-field model of nuclear matter. I found that the mean-field description yields fairly good results which look quite consistent with the skewness and the kurtosis measured in the beam-energy scan.

Because the mean-field approximation is based on the quasiparticle treatment, in fact, it is not much different from the hadron resonance gas model except for the interaction effects incorporated in terms of the scalar and the vector mean fields. I numerically checked that the kurtosis is suppressed at smaller collision energy (i.e., higher baryon density) due to the vector mean field, which is directly coupled to the baryon density. I would emphasize that my main point is to draw attention to a realistic possibility to interpret the BES data as an extrapolation from nuclear matter, and not to make a serious comparison between models and the experimental data. To this end I need to take account of canonicalness in a finite volume [36] and also diffusion effects in rapidity subspace [37].

Finally, in the present study, I discuss the effects of isospin correlations and reach the conclusion that such effects are only minor such that I can ignore them in the first approximation. Even in the case of strong residual interactions that realize complete randomization in isospin space, I find that the deviation from the HRG prediction is at most 10% at the smallest collision energy of a few GeV. Therefore, for a semiquantitative estimate, I can simply identify the proton number fluctuations as (half of) the baryon number fluctuations.

In this paper I only mentioned another possibility of flavor mixing through the off-diagonal susceptibility χ_{ud}. This nonzero χ_{ud} arises from the pion dynamics, so it is quite nontrivial how we relate χ_{ud} to the correlations purely among the proton number N_p and the neutron number N_n. I am now making progress in this direction in order to refine relationship between $\chi_p^{(n)}$ and $\chi_B^{(n)}$.

Although the σ-ω model is one of the simplest methods to capture the essential features of nuclear matter, it would be more desirable to develop quantitative investigations by means of more systematic approaches such as the chiral perturbation theory. It would be definitely worth attempting the fully quantitative comparisons for $S\sigma$ and $\kappa\sigma^2$ within the framework of the chiral perturbation theory and also more established Bruckner-type calculations. This is one of my future problems and the results shall be reported in followups hopefully soon.

ACKNOWLEDGMENTS

The author thanks Masayuki Asakawa and Masakiyo Kitazawa for useful discussions. This work was supported by MEXT-KAKENHI Grant No. 24740169.

[1] P. Braun-Munzinger and J. Wambach, Rev. Mod. Phys. **81**, 1031 (2009).

[2] K. Fukushima and T. Hatsuda, Rept. Prog. Phys. **74**, 014001 (2011); K. Fukushima, J. Phys. G **39**, 013101 (2012);

K. Fukushima and C. Sasaki, Prog. Part. Nucl. Phys. **72**, 99 (2013).
[3] G. Aarts, PoS LATTICE **2012**, 017 (2012).
[4] R. Fukuda, K. Fukushima, T. Hayata, and Y. Hidaka, Phys. Rev. D **89**, 014508 (2014).
[5] M. A. Stephanov, K. Rajagopal, and E. V. Shuryak, Phys. Rev. Lett. **81**, 4816 (1998); Phys. Rev. D **60**, 114028 (1999).
[6] K. Fukushima, Phys. Rev. D **78**, 114019 (2008).
[7] E. Nakano and T. Tatsumi, Phys. Rev. D **71**, 114006 (2005).
[8] D. Nickel, Phys. Rev. Lett. **103**, 072301 (2009).
[9] K. Fukushima, Phys. Rev. D **86**, 054002 (2012).
[10] For a review, see M. Buballa and S. Carignano, Prog. Part. Nucl. Phys. **81**, 39 (2015).
[11] L. Adamczyk *et al.*, STAR Collaboration, Phys. Rev. Lett. **112**, 032302 (2014).
[12] M. A. Stephanov, Phys. Rev. Lett. **102**, 032301 (2009).
[13] M. Asakawa, S. Ejiri, and M. Kitazawa, Phys. Rev. Lett. **103**, 262301 (2009).
[14] J. Cleymans, H. Oeschler, K. Redlich, and S. Wheaton, Phys. Rev. C **73**, 034905 (2006).
[15] F. Becattini, J. Manninen, and M. Gazdzicki, Phys. Rev. C **73**, 044905 (2006).
[16] A. Andronic, P. Braun-Munzinger, and J. Stachel, Phys. Lett. B **673**, 142 (2009); **678**, 516 (2009).
[17] S. Borsanyi, G. Endrodi, Z. Fodor, C. Hoelbling, S. Katz, S. Krieg, C. Ratti, and K. Szabo, J. Phys.: Conf. Ser. **336**, 012019 (2011).
[18] F. Karsch and K. Redlich, Phys. Lett. B **695**, 136 (2011).
[19] J. Stachel, A. Andronic, P. Braun-Munzinger, and K. Redlich, J. Phys.: Conf. Ser. **509**, 012019 (2014).
[20] T. Tatsumi, N. Yasutake, and T. Maruyama, arXiv:1107.0804.
[21] S. Floerchinger and C. Wetterich, Nucl. Phys. A **890-891**, 11 (2012).
[22] J. D. Walecka, Ann. Phys. (NY) **83**, 491 (1974).
[23] M. Drews, T. Hell, B. Klein, and W. Weise, Phys. Rev. D **88**, 096011 (2013).
[24] A. Andronic *et al.*, Nucl. Phys. A **837**, 65 (2010).
[25] K. Fukushima, Phys. Rev. D **79**, 074015 (2009).
[26] M. Buballa, Nucl. Phys. A **611**, 393 (1996).
[27] J. P. Blaizot, Phys. Rep. **64**, 171 (1980).
[28] T. Sasaki (private communication).
[29] P. Chomaz, arXiv:nucl-ex/0410024.
[30] R. V. Gavai and S. Gupta, Phys. Rev. D **73**, 014004 (2006); **78**, 114503 (2008).
[31] S. Mukherjee, M. G. Mustafa, and R. Ray, Phys. Rev. D **75**, 094015 (2007).
[32] M. Cristoforetti, T. Hell, B. Klein, and W. Weise, Phys. Rev. D **81**, 114017 (2010).
[33] K. Fukushima, Phys. Lett. B **591**, 277 (2004).
[34] E. Megias, E. Ruiz Arriola, and L. L. Salcedo, Phys. Rev. D **74**, 065005 (2006).
[35] M. Kitazawa and M. Asakawa, Phys. Rev. C **85**, 021901 (2012); **86**, 024904 (2012); **86**, 069902 (2012).
[36] A. Bzdak, V. Koch, and V. Skokov, Phys. Rev. C **87**, 014901 (2013).
[37] M. Sakaida, M. Asakawa, and M. Kitazawa, Phys. Rev. C **90**, 064911 (2014).